Journal of Electronic Imaging

SPIEDigitalLibrary.org/jei

Interpolating vertical parallax for an autostereoscopic three-dimensional projector array

Andrew Jones
Koki Nagano
Jing Liu
Jay Busch
Xueming Yu
Mark Bolas
Paul Debevec

Journal of Electronic Imaging 23(1), 011005 (Jan–Feb 2014)

Interpolating vertical parallax for an autostereoscopic three-dimensional projector array

Andrew Jones,[a,*] Koki Nagano,[a] Jing Liu,[a,b] Jay Busch,[a] Xueming Yu,[a] Mark Bolas,[a] and Paul Debevec[a]
[a]USC Institute for Creative Technologies, 12015 Waterfront Drive, Playa Vista, California 90094
[b]University of Santa Cruz, Computer Science, 1156 High Street, Santa Cruz, California 95064

Abstract. We present a technique for achieving tracked vertical parallax for multiple users using a variety of autostereoscopic projector array setups, including front- and rear-projection and curved display surfaces. This hybrid parallax approach allows for immediate horizontal parallax as viewers move left and right and tracked parallax as they move up and down, allowing cues such as three-dimensional (3-D) perspective and eye contact to be conveyed faithfully. We use a low-cost RGB-depth sensor to simultaneously track multiple viewer head positions in 3-D space, and we interactively update the imagery sent to the array so that imagery directed to each viewer appears from a consistent and correct vertical perspective. Unlike previous work, we do not assume that the imagery sent to each projector in the array is rendered from a single vertical perspective. This lets us apply hybrid parallax to displays where a single projector forms parts of multiple viewers' imagery. Thus, each individual projected image is rendered with multiple centers of projection, and might show an object from above on the left and from below on the right. We demonstrate this technique using a dense horizontal array of pico-projectors aimed into an anisotropic vertical diffusion screen, yielding 1.5 deg angular resolution over 110 deg field of view. To create a seamless viewing experience for multiple viewers, we smoothly interpolate the set of viewer heights and distances on a per-vertex basis across the array's field of view, reducing image distortion, cross talk, and artifacts from tracking errors. *© 2014 SPIE and IS&T* [DOI: 10.1117/1.JEI.23.1.011005]

Keywords: computer graphics; displays; tracking; three-dimensions; projector array; autostereoscopic; parallax; multiple centers of projection.

Paper 13487SSP received Aug. 31, 2013; revised manuscript received Dec. 11, 2013; accepted for publication Jan. 7, 2014; published online Mar. 5, 2014.

1 Introduction

Autostereoscopic displays hold the promise of seamless three-dimensional (3-D) imagery that can be seen from any viewpoint without the need for special 3-D glasses. The fundamental obstacle is finding new ways to redirect pixels in different angular directions in order to be seen by multiple viewers. Unfortunately, full-motion parallax comes at a high cost as the total pixel count needed by a display is directly proportional to the number of viewers. Traditionally, a 3-D display with 10 horizontal views requires 10 times the number of pixels as a similar two-dimensional (2-D) display, but a display with 10 horizontal and vertical views requires 100 times the pixels. As a result, most autostereoscopic displays are limited to horizontal parallax only (HPO), where the image does not change as the height of the viewer changes. This is a reasonable tradeoff as human movement is dominated by horizontal motion. Yet, it is still desirable to handle multiple users with varying physical heights, and occasional changes in vertical parallax as users approach the display, jump, or crouch.

Projector arrays are well suited for 3-D displays because of their ability to generate dense and steerable arrangements of pixels. As video projectors continue to shrink in size, power consumption, and cost, it is now possible to closely stack projectors so that their lenses are almost continuous. We present a new HPO display utilizing a single dense row of projectors. A vertically anisotropic screen turns the glow of each lens into a vertical stripe while preserving horizontal angular variation. The viewer's eye perceives several vertical stripes from multiple projectors that combine to form a seamless 3-D image. Rendering to such a display requires the generation of multiple center of projection (MCOP) imagery, as different projector pixels diverge to different viewer positions. Previously, Jones et al.[1,2] proposed an MCOP rendering solution in the context of high-speed video projected onto a spinning anisotropic mirror. A front-mounted projector array may be seen as an unfolded spinning mirror display where each high-speed frame corresponds to a different discrete projector position. In this paper, we extend this framework for use with both front- and rear-projection 3-D projector arrays.

As every viewer around an HPO display perceives a different 3-D image, it is possible to customize each view with a different vertical perspective. Such a setup has the unique advantage that every viewer can have a unique height while experiencing instantaneous horizontal parallax. The problem is to create a continuous estimate of viewer height and distance for all potential viewing angles given only a sparse set of tracked viewer positions. This estimate must provide consistent vertical perspective to both tracked and untracked viewers. The set of viewers is dynamic, and it is possible that the tracker will miss a viewer particularly as viewers enter or leave the viewing volume. Previous techniques for rendering MCOP images for autostereoscopic displays[1,2] assume a constant viewer height and distance for each projector frame. In practice, this limitation can result in visible

*Address all correspondence to: Andrew Jones, E-mail: gl@usc.ict.edu

distortion, image tearing, and cross talk where a viewer sees slices of multiple projector frames rendered with inconsistent vertical perspective. This is especially visible when two viewers are close together but have different heights. We solve this problem by dynamically interpolating multiple viewer heights and distances within each projector frame as part of a per-vertex MCOP computation. We then compare the performance of different interpolation functions. Our algorithm can handle both flat screens as well as convex mirrored screens that further increase the ray spread from each projector.

Our primary contributions are:

1. An autostereoscopic 3-D projector array display built with off-the-shelf components.
2. A new per-vertex projection algorithm for rendering MCOP imagery on standard graphics hardware.
3. An interpolation algorithm for computing multiple vertical perspectives for each projector.
4. An analysis of curved mirrored screens for autostereoscopic projector arrays.

2 Related Work

Many different forms of glasses-free displays have been developed over the last century, and good surveys[3] exist covering emerging 3-D display technologies. We will focus on the development of screen materials, projector arrays, and user tracking that pertain to our system.

As early as 1931, Ives[4] demonstrated that a lenticular screen composed of vertically aligned cylindrical lenses could be used to generate autostereoscopic 3-D imagery. Originally a special photograph with alternating left and right eye stripes was mounted directly behind the screen. The multiple stripes behind each vertical cylindrical lens diverge to different horizontal views. Today, due to their relative low cost, LCDs with vertical lenticular lenses remain the most common form of autostereoscopic display. As the number of views is limited by the pixel pitch of the backing image or LCD, Ives showed that increased stripe density could be achieved by focusing 39 film projectors onto a retroreflective or diffuse screen behind the lenticular array. A similar idea was used by Matusik and Pfister,[5] who presented real-time acquisition, transmission, and display using 16 digital projectors and a vertically aligned lenticular screen. In both cases, the light is focused onto a diffuse plane behind the lenticular array then redistributed by each cylindrical lens. As with Ives, the horizontal angular variation still comes from the specific shape and focal length of the lenticular array. Even with additional projector resolution, nearly all vertically aligned lenticular displays have limited horizontal field of view as the lenticular cylinders start to self-occlude.

If the cylindrical lenticular lenses are aligned horizontally then they function as a vertical anisotropic diffuser. Instead of bending light in the horizontal axis, a horizontal cylindrical lens scatters each incoming ray into a vertical plane. This orientation allows for greater angular density as it preserves the angular variation of the original projector spacing. Unlike Ives and Matusik and Pfister,[5] the exact focal length of the lenticular screen is not critical as long as the vertical diffusion encompasses all viewers. Based on this principle, the commercial company Holografika has demonstrated large-format projector arrays including the rear-projection HoloVizio 720RC[6] and the front-projection HoloVizio C80.[7] Recently, Kawakita et al.[8] designed a massive 5-m rear projection display. Both Holografika and Kawakita et al. displays are built using large projector units with wide spacing. Additional optics are added to their screens to refocus and redirect projector rays across a narrow horizontal field of view. Yoshida et al.[9] have developed an array with 103 micro-LCD projectors as a glasses-free tabletop 3-D display. The projectors illuminate a conical anisotropic screen coupled with a holographic diffuser situated below the table surface. The drawback of this form factor is that virtual objects on or above the table surface will always appear blurred as they are outside the depth of field of the display. A more in-depth comparison with these projector arrays can be found in Table 1.

User tracking has long been used for single-user displays with stereoglasses[10–12] and single-user autosteroscopic displays[13] in order to update both horizontal and vertical motion parallax. Our system is the first autostereoscopic projector array to incorporate tracking of multiple users for vertical parallax. Our method has the advantage that a large number of users still perceive instantaneous horizontal parallax. Tracking latency is less noticeable as it is restricted to the vertical axis where rapid movements are less frequent. None of these existing lenticular or projector arrays generate vertical parallax although our technique could also be implemented for these and other autosteroscopic displays.

3 Apparatus

Our projector array system consists of 72 Texas Instruments DLP Pico projectors each of which has 480×320 resolution. At the time of publication, these projectors are the smallest commercially available projector as they do not include additional battery or processing hardware. Other LCoS or MEMS-based projector technologies could also be produced in a similar size. Even though the projectors use low-power LED light source, additional fans were added to provide active cooling. Our projectors are evenly spaced along a 124-cm circular curve with a radius of 60 cm. This setup provides an angular resolution of 1.66 deg between views. At the center of the circle, we place a 30×30 cm vertically anisotropic screen (see Fig. 1). The ideal screen material should have a wide-vertical scattering profile so the 3-D image can be seen from multiple heights, and a narrow horizontal scattering profile that maintains the divergence of different projector pixels to varying horizontal views. When a projected image passes through the vertically anisotropic screen, it forms a series of vertical stripes. Without any horizontal diffusion, the stripe width is equivalent to the width of the projector lens.

Each projector is 1.42-cm wide with a 4-mm lens. In order to eliminate any gap between stripes, this would require stacking several hundred projectors in overlapping vertical rows.[14] We found that acceptable image quality could be achieved with a single row of projectors if we use a holographic diffuser to generate 1 to 2 deg of additional horizontal diffusion and stack the projectors with a 2-mm gap (see Fig. 2 and Video 2 at 0:30). The holographic diffuser generates a slight angular blur to the projector rays, smoothly filling in the gaps between the projectors with adjacent pixels. Ideally, the width of the diffusion lobe should be equal to

Table 1 Comparison of our system specifications with other autostereoscopic projector arrays.

	Matusik and Pfister (Ref. 5)	HoloVizio 720RC	Kawakita et al. (Ref. 8)	Yoshida et al. (Ref. 9)	Our system
Angular resolution	1.88 deg	Unknown	0.24 deg	1.27 deg	1.66 deg
Horizontal diffusion	N/A	Unknown	0.88 deg	0.5 to 1 deg	1 to 2 deg
Vertical diffusion	N/A	Unknown	35 deg	60 deg	60 deg
Horizontal field of view	30 deg	40 deg	13.5 deg	130 deg	118 deg
Horizontal screen size	1.8 m	3 m	5 m	20 cm	30 cm
Screen shape	Flat	Flat	Flat	Cone/cylinder	Flat/convex
Form-factor	Front/rear	Rear	Rear	Tabletop	Front/rear
Number of projectors	16	80	57	103	72
Projector distance	Unknown	5.5 m	5.5 m	80 cm	60 cm
Number of computers	8	4	Unknown	6	1
Vertical parallax	No	No	No	No	Yes, with tracking

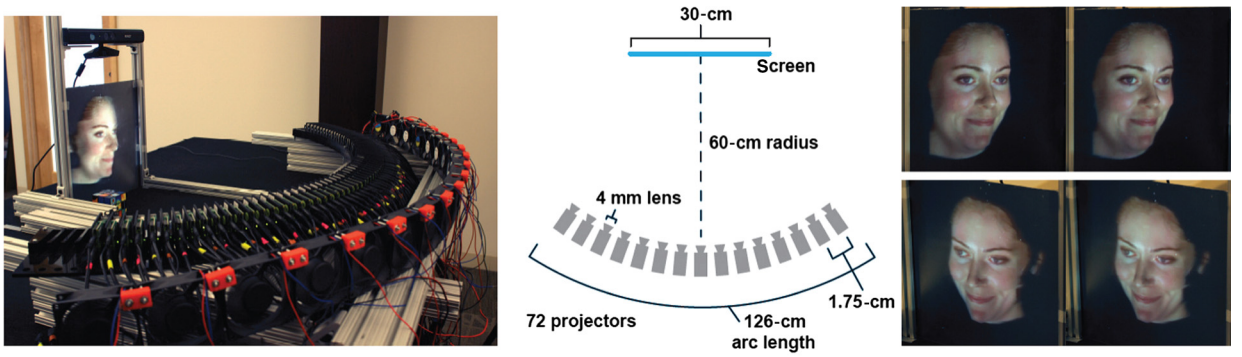

Fig. 1 (a) A three-dimensional (3-D) face is shown on our autosteroscopic 3-D projector array. The display combines both autostereoscopic horizontal parallax with vertical tracking to generate different horizontal and vertical views simultaneously over a full 110-deg field of view. (b) Diagram showing the dimensions of the display. (c) 3-D stereophotographs of a human face. The stereopairs are left–right reversed for cross-fused stereoviewing.

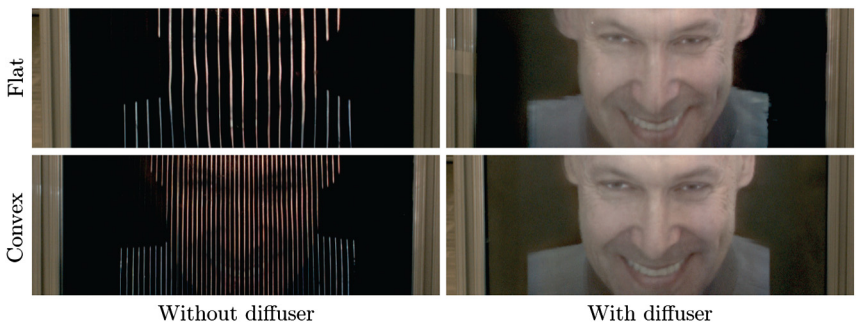

Fig. 2 The anisotropic screen forms a series of vertical lines, each corresponding to a projector lens. A 1- to 2-deg horizontal diffuser is used to blend the lines and create a continuous image. The top rows show stripes and imagery reflected on a flat anisotropic screen. The bottom row shows imagery reflected on a convex anisotropic screen. By varying the curvature of a mirrored anisotropic screen, we can decrease the pitch between reflected projector stripes. This increases the spatial resolution at the screen depth at the expense of overall angular resolution and depth of field.

Video 1 Video comparison of imagery displayed on front and rear-projection anisotropic screens (ASV, 79 KB) [URI: http://dx.doi.org/10.1117/1.JEI.23.1.011005.1].

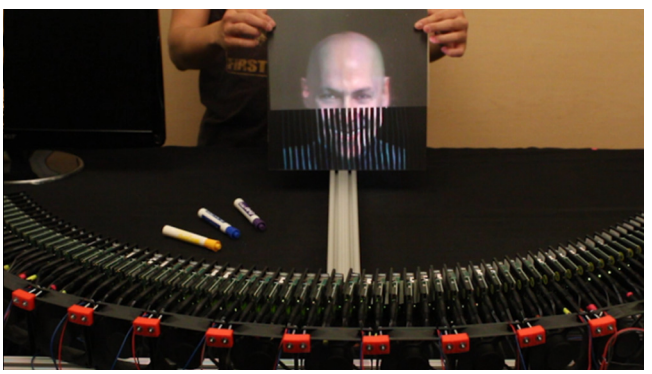

Video 2 Video shows the placement of a narrow holographic diffuser to fill gaps between projectors (MOV, 2.52 MB) [URI: http://dx.doi.org/10.1117/1.JEI.23.1.011005.2].

the angle between projectors lens, though in practice, we are limited to commercially available scattering profiles which typically come in 1-deg increments.

For rear-projection setups, we use a horizontally aligned lenticular sheet layered with an anisotropic holographic diffuser with a horizontal 2-deg and vertical 60-deg scattering profile (see Fig. 3 and Video 1 at 0:14). Alternatively for front-projection, we reflect off a fine lenticular screen behind the holographic diffuser (see Fig. 1 and Video 1 at 0:20). The lenticular screen is painted matte black on the reverse flat side to reduce ambient light and improve black levels. As the light passes twice through the diffuser, only 1 deg of additional horizontal diffusion is required. All our screen components are currently available off-the-shelf. The holographic diffusers are from Luiminit Co, (Torrance, California). The lenticular material is a 60 lpi 3-D60 plastic screen from Microlens Technology, (Indian Trail, North Carolina). We also explored other anisotropic screen materials. For example, finely brushed aluminum or steel can be highly anisotropic with similar vertical and horizontal scattering suitable for a reflective front-projection screen.[2] Brushed metal is widely available and inexpensive. However, in an experimental comparison, we found that brushed metal generally produces a lower contrast ratio than a front-surface lenticular reflection.

The amount of horizontal holographic diffusion also influences the perceived resolution of the display. It is preferable to stack projectors as closely as possible to increase the horizontal spatial and angular resolutions. The image seen by each viewer is composed of vertical stripes from multiple projectors. Smaller gaps between stripes mean higher horizontal spatial resolution. As the amount horizontal diffusion increases, the gaps are filled with blurred pixel information from adjacent angular rays. This effectively increases the horizontal resolution at the expense of angular resolution.

We drive our projector array using a single standard Windows computer with no special memory or CPU. The only requirement is that the motherboard can accommodate four graphics cards. We use four ATI Eyefinity graphics cards with a total of 24 video outputs. The CPU is primarily used for user-tracking; all other operations are performed on the GPU. The animations shown in the video used around 5000 triangles and ran at 100 to 200 fps on an ATI Eyefinity 7800. To achieve maximum performance, rendering is distributed across all four graphics cards. As not all graphics libraries provide this low level control, we explicitly create a different application and render context per GPU, with the different instances synchronized through shared memory. The main bottleneck is frontside bus data transfer as textures and geometry need to be uploaded to all GPUs. We then split each video signal using 24 Matrox TripleHeadToGo video splitters, each of which supports three HDMI outputs. This allows for a maximum of 72 tiled video signals. We use DisplayFusion desktop manager software to handle the multimonitor setup.

To track viewer positions, a Microsoft Kinect camera is mounted directly above the screen. The depth camera is ideal as it provides both viewer height and distance. The Kinect device does have some built-in latency around 100 ms. To get a more robust position, we track both the body's center of mass and facial features with Kinect API. We implement

(a) (b)

Fig. 3 (a) Photograph of our rear-mounted projector array setup. (b) Photograph of the calibration setup for front-mounted projector array. To compute relative projector alignment, we sequentially correspond a virtual AR marker generated by each projector with a printed AR marker.

an additional Kalman filter to further smooth the positional data and estimate tracking confidence. The output of the Kinect tracker along with the corresponding interpolated viewer heights can be seen in Video 3. The current Kinect API is limited to tracking six active users. However, our interpolation method would easily work with other 3-D tracking methods.

4 Calibration

Even with a machined projector mount, there is still noticeable geometric and radiometic variation between projectors. We automate the geometric calibration of the projectors using a 2-D rectification process to align projector images to the plane of the screen. We first place a diffuse surface in front of the screen, then sequentially project and photograph an AR marker from each projector[15] (see Fig. 3). We then compute a 2-D homography matrix that maps the detected marker corners in each projector to a physical printed marker also attached to the screen. At the same time, we measure the average intensity of light from each projector on the diffuse surface and compute a per-projector scale factor to achieve consistent brightness and color temperature across the entire projector array. Although there is some variation between projectors, the LED light source for each projector is relatively stable over time.

5 Viewer Interpolation

As described above, anisotropic screens do not preserve a one-to-one mapping between projectors and views, as projector rays diverge to multiple viewers at potentially different angles, heights, and distances. To generate an image that can be viewed with a single perspective, we must render MCOP images that combine multiple viewing positions. A brute force solution would be to prerender out a large number of views with regular perspective and resample these images based on the rays generated by the device as done by Rademacher et al.[16] A variant of this technique was implemented by Jones et al.[1] for existing photographic datasets. However, resampling introduces a loss of resolution.

For scenes with known geometry, an alternative approach is to replace the standard perspective projection matrix and directly render MCOP images. We define this MCOP operation so that it maps each 3-D vertex point to 2-D projector coordinates based on a different viewing transformation.

Video 3 Two viewers are tracked by the Microsoft Kinect depth camera. The graph shows the continuous estimate of viewer height that is interpolated using a smooth Gaussian falloff function (MOV, 16.3 MB) [URI: http://dx.doi.org/10.1117/1.JEI.23.1.011005.3].

This per-vertex geometric warp can capture smooth distortion effects and can be efficiently implemented in a standard GPU vertex shader. Our method is based on a similar approach was used by Jones et al.[1] to generate MCOP renders.

The first step is to project each 3-D vertex onto the screen. For each vertex (Q), we trace a ray from the current projector position (P) through the current vertex (Q). We intersect this first ray (PQ) with the screen surface to find a screen point (S_P). The second step is to compute a viewing position associated with this vertex. The set of all possible viewers can be represented as a continuous manifold spanning multiple heights and distances. In the general case, the intersection of the ray (PQ) with this manifold defines the current corresponding viewer (V). Finally, we trace a second ray from the viewer (VQ) back to the current vertex (Q) and intersect with the screen a second time (S_V). The actual screen position uses the horizontal position of S_P and the vertical position of S_V. This entire process can be implemented in a single GPU vertex shader. In essence, the horizontal screen position is determined by projecting a ray from the projector position, while the vertical screen position is based on casting a ray from the viewer position. The difference in behavior is due to the fact that the anisotropic screen acts as a diffuse surface in the vertical axis. We multiply the final screen position by the current calibrated projector homography to find the corresponding projector pixel position for the current vertex.

In practice, it is not easy to define the manifold of viewer positions as we only know a few sparse tracked positions. We propose a closed-form method for approximating this manifold as a series of concentric rings. In 2007, Jones et al.[1] assumed that the viewing height and distance was constant for all projectors. This arrangement corresponds to a single circle of potential viewers. As the viewers are restricted to lie on this circle, the viewpoints represented by each rendered MCOP image vary only in their horizontal angle, with no variation in height and distance. One trivial extension would be to interpolate viewer height and distance once per projector frame and adjust the radius of the viewing circle. In our comparison images, we refer to this method as per-projector interpolation. However when tracking multiple viewers close together, it is possible for the viewing height to change rapidly within the width of a single MCOP projector frame.

We solve this issue by interpolating the viewer height and distance per-vertex. We pass the nearest two tracked viewer positions to the vertex shader. Each viewer height and distance defines a cylinder with a different viewing radius. We then intersect the current projector-vertex ray (PQ) with both cylinders. To determine the final viewing position for this ray, we compute a weighted average of the two viewer heights and distances. The interpolation weights of each tracked viewer position are a function of the angle (θ_1, θ_2) between the cylinder intersection and the original tracked point. A top-down view of these intersections is shown on the left side of Fig. 4. When computing the weighted average, we also add a third default value with very low weight. This value corresponds to the average user height and distance appropriate for untracked viewers. As the viewer's angle from each tracked point increases, the influence of the point decays and the viewer returns to the default height and distance [Fig. 4(b)]. We implemented two different

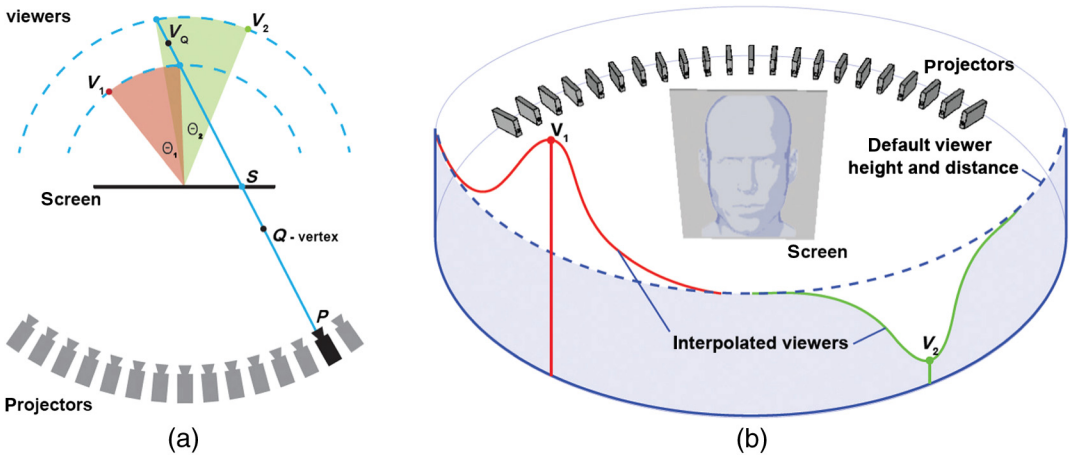

Fig. 4 (a) Diagram showing how we compute the corresponding viewing position for each vertex by tracing a ray from the projector position P through the vertex Q. We intersect the ray with the screen to find the horizontal screen position S. We intersect the ray with viewing circles defined by the nearest two tracked viewers (V_1, V_2). We interpolate between the tracked viewer positions based on their angular distance from the intersection points. (b) Diagram showing the continuous curve formed by the interpolated viewer positions. The curve returns to a default viewer height and distance away from tracked viewer positions (V_1, V_2).

Table 2 Vertex shader pseudocode that projects a 3-D scene vertex into 2-D screen coordinates as described in Sec. 5. The code interpolates between multiple tracked viewer positions per vertex. It assumes that helper functions are defined for basic geometric intersection operations.

```
// project 3D vertex positions to 2D screen coordinates using MCOP warp
void warpVertex(
  float3 Q : POSITION,          // input 3D vertex position
  uniform float3x3 Homography   // 2D projector homography
  uniform float4 P,             // current projector position
  uniform float3 T[],           // tracked viewers positions
  uniform float C[],            // tracked viewer confidences
  out float3 oQ : POSITION)     // output 2D screen coordinate
{
  P = computeProjectorPostion(P);       // use reflected projector position if front-projection screen
  V = interpolateViewer(Q, P, V, T, C); // find viewer that sees current vertex from current projector
  float3 VQ = V - Q;                    // define ray from viewer position V to vertex Q
  float3 S = intersectRayWithScreen(VQ) // intersect with planar or cylindrical curved screen
  oQ = mul( Homography, S );            // apply projector homography to screen coordinate
}

// interpolate tracked viewer positions per-vertex
float3 interpolateViewer(float3 Q, float3 P, float3 V, float3[] T, float[] C) {
  float sum_of_weights;
  float current_viewer;
  float3 PQ = Q - P;                    // define ray from reflected projector position P to vertex Q
  for each tracked viewer t
  {
    float3 I = intersectRayWithCylinder(PQ, radius(t)); // radius of cylinder is tracked viewer distance
    float angle = computeAngle(T, I);                   // compute angle between intersection and tracked viewer
    float weight = falloffFunction(angle);              // falloff function could be Gaussian or Hat function
    weight *= C[t];                                     // also weight by tracking confidence
    current_viewer += t * weight;
    sumWeight += weight;
  }
  current_viewer += default_weight * default_viewer;    // add in default viewer
  sumWeight += default_weight;                          // with low default weight
  return currentViewer / sumWeight;                     // compute weighted average of tracked viewer positions
}
```

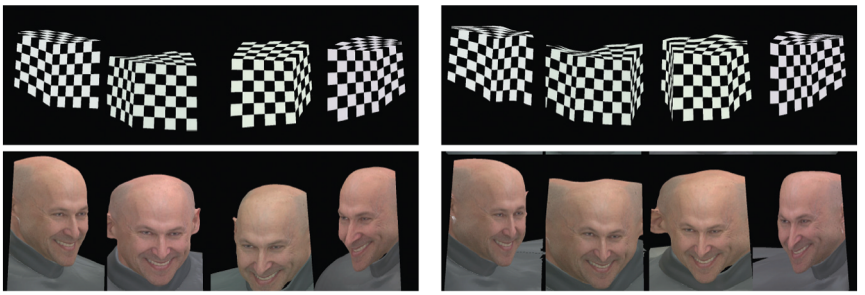

Fig. 5 Our algorithm renders out a different MCOP image for each of 72 projectors. This is a sampling of the generated images using per-vertex vertical parallax blending with a Gaussian falloff function. Each image smoothly blends between multiple horizontal and vertical viewer positions, which gives the appearance of an unwrapped object. Flat front and rear projection screens produce almost identical imagery. Convex screens have additional warping as each projector spans a wider set of viewers.

falloff functions centered around each track point—a normalized Gaussian and a constant step hat function. The Gaussian function smoothly decays as you move away from a tracked viewer position, while the hat function has a sharp cutoff. A comparison of the two interpolation functions is included in Sec. 7. The weight function can be further modulated by the confidence of the given tracked viewer position. This decay makes the system smoothly adjust to viewers missed by the tracking system or new viewers that suddenly enter the viewing volume. Pseudocode for computing per-vertex projection and viewer interpolation can be found in Table 2. The final rendered frames appear warped as different parts of each frame smoothly blend between multiple horizontal and vertical perspectives. Figure 5 shows a subset of these MCOP frames before they are sent to the projector.

A related MCOP rendering algorithm was also proposed by Jones et al.[2] In this later work, the entire per-vertex projection operator from 3-D vertices to 2-D projector positions was precomputed as a six-dimensional lookup table based on 3-D vertex position, mirror angle, and viewer height and distance. The lookup table was designed to handle more complex conical anisotropic reflections that occur when the projector rays are no longer perpendicular to the mirror's vertical anisotropic axis. For projector arrays, we found that rays scattered by the screen remained mostly planar with very little conical curvature. Furthermore, the lookup table's height and distance was indexed based on a single reflection angle per projector frame. This assumption is analogous to our per-projector interpolation examples. Instead of modeling different heights and distances for each projector, Jones et al. used a concave anisotropic mirror to optically refocus the projector rays back toward a single viewer. Such an approach would not work for a rear-mounted projector array where there is no mirror element. Our software solution is more general and allows for a wider range of screen shapes.

6 Convex Screen Projection

For a front-mounted array, the pitch between reflected stripes can also be reduced by using a convex reflective anisotropic screen. The convex shape magnifies the reflected projector positions so they are closer to the screen, with narrower spacing, and a wider field of view (Fig. 2). As less horizontal diffusion is required to blend between stripes, objects at the depth of the screen have greater spatial resolution. This improved spatial resolution comes at the cost of angular resolution and lower spatial resolution further from the screen. Zwicker et al.[17] provide a framework for defining the depth of field and display bandwidth of anisotropic displays. For a given initial spatial and angular resolutions, the effective spatial resolution is halved every time the distance from the screen doubles. In Fig. 6, we plot the tradeoff between spatial resolution and depth of field given the initial specifications of our projector prototype. A curved mirror is also preferable for 360-deg applications, where an anisotropic cylinder can be used to reflect in all directions without any visible seams.

As a convex mirror effectively increases each projector's field of view, each projector frame must represent a wider range of viewer positions. It becomes more critical to compute multiple viewer heights per projector frame. To directly render MCOP frames, we use the flat screen projection algorithm from the previous section with two minor modifications. For front-mounted projection setups that use a mirrored anisotropic screen, we first unfold the optical path to find reflected projector positions. The rays reflected off a convex mirror do not always reconverge at a single

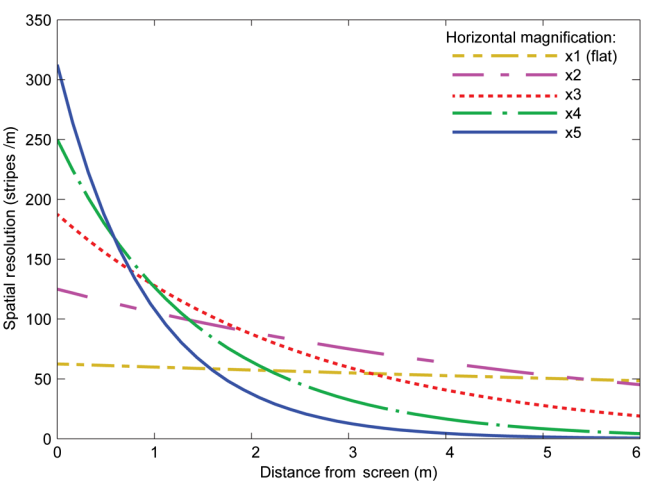

Fig. 6 Graph showing tradeoff between spatial magnification using convex mirrored screens and depth of field. Greater mirror curvature increases density of projector stripes and spatial resolution at the screen; however, spatial resolution falls off rapidly away from the screen.

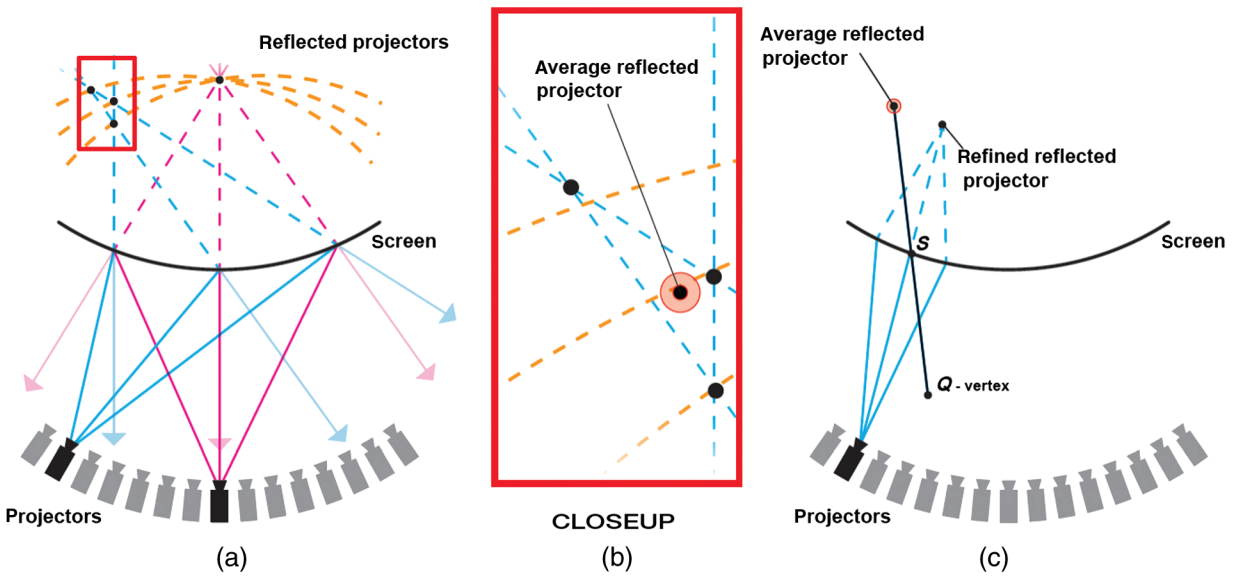

Fig. 7 (a) For a convex mirrored screen, reflected projector rays no longer converge on a single projector position. (b) We sample multiple points on the mirror surface and compute an average reflected projector position for each real projector. (c) We then iteratively refine by reflected position per vertex by tracing a ray from the average position through the vertex to the convex screen. We then compute a more accurate reflected position based on the local neighborhood of the screen point.

reflected projector position (Fig. 7, right). A first-order approximation is to sample multiple reflected rays and average the resulting intersection points (Fig. 7, center). This can still result in distortion for extreme viewing angles. A more accurate solution is to compute a different projector position per-vertex. In the per-vertex variant, we use the average reflected projector to compute an initial intersection point with the screen. We then interpolate a second, more accurate reflected projector position based on the local curvature around this screen point (Fig. 7, right). This process could be iterated to further refine the reflected projector position, though in our tests the reflected rays converged in a single iteration. Second, we discard rays that reflect off the convex mirror near grazing angles, as these regions are extremely distorted and are very sensitive to small errors. In comparison to a flat screen, a convex screen requires rendered frames covering a wider variation of views and greater per-vertex warping (Fig. 5). Video 4 shows vertical parallax on a curved front-projection screen

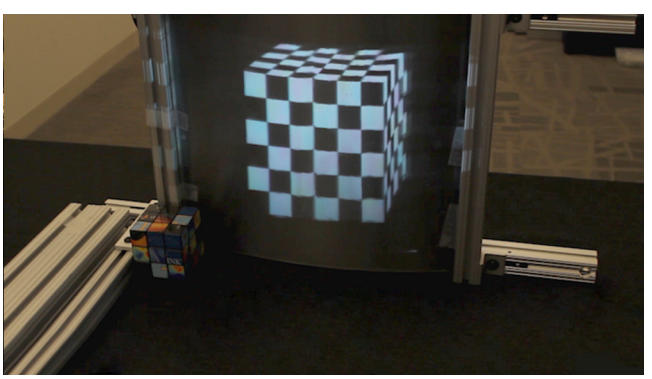

Video 4 Vertical parallax is shown for a tracked viewer and a curved front-projection screen. The reflected projector positions are iteratively refined to correct for the mirror shape (MOV, 2.66 MB) [URI: http://dx.doi.org/10.1117/1.JEI.23.1.011005.4].

7 Results

Our display can generate stereo and motion parallax over a wide field of view. Although it is difficult to communicate the full 3-D effect with 2-D figures, Fig. 1 shows several stereophotographs printed for cross-fuse stereoviewing. The motion parallax can also be seen throughout the accompanying video.

To evaluate our view interpolation algorithms, we render multiple geometric models from a variety of heights and distances (Fig. 8). We use a checkered cube to identify any changes in perspective or warping and a spherical model of the Earth to illustrate correct aspect ratio. We also show two high-resolution face models as examples of organic shapes. We then photograph the display from three views: a lower left view, a center view, and a high right view. We measure the real camera positions and render matching virtual views to serve as ground-truth validation (Fig. 8, row 1). With no vertical tracking, the display only provides horizontal parallax and all viewers will see a foreshortened image as they move above or below the default height (row 2). Note that the top and bottom faces of the cube are never visible and the eye gaze for the face is inconsistent. If we enable tracking for the left and right cameras (rows 3 to 6), then it is possible to look up and down at the objects.

Also in Fig. 8, we compare our new interpolation algorithm for handling multiple different viewers. For rows 2 and 3, we compute a per-vertex viewer height and distance as described in Sec. 5. Per-vertex vertical parallax interpolation produces plausible and consistent perspective across the entire photographed view. In contrast, rows 4 and 5 demonstrate interpolation that uses a constant viewer height and distance per projector. Each projector still interpolates the nearest two tracked viewer positions; however, the interpolation weights are uniform across all vertices. Per-projector interpolation generates significant distortion for all three views where the vertical perspective on the left side of the image does not match the perspective on the right side.

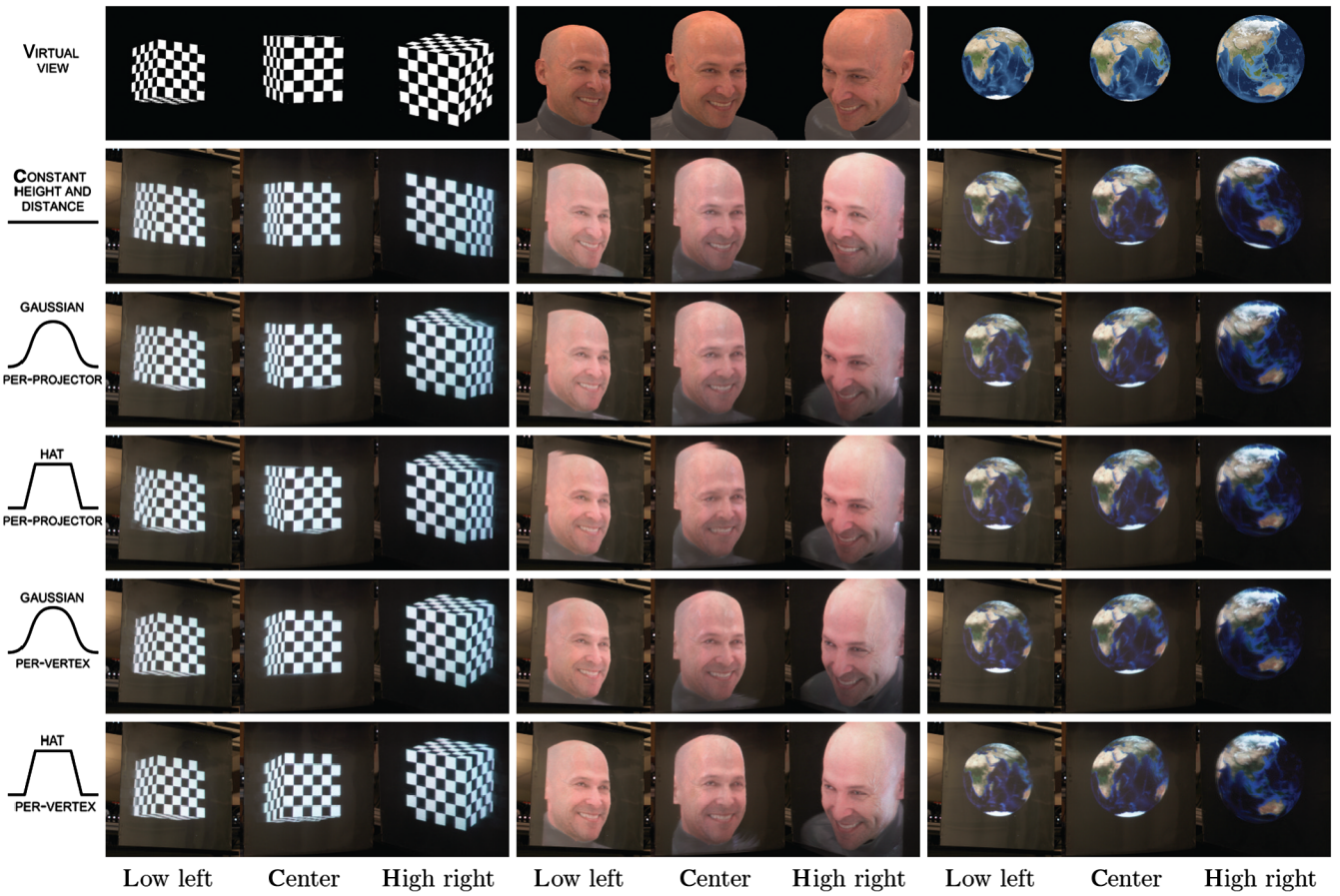

Fig. 8 This figure shows three virtual objects viewed by an untracked center camera and two tracked left and right cameras. As a ground-truth comparison, we calibrate the positions of three cameras and render out equivalent virtual views of the objects (first row), while the remaining rows show photographs of the actual display prototype. If a single constant viewer height and distance are used then the viewer sees significant foreshortening from high and low views (second row). We also compare different viewer interpolation functions for interpolating multiple viewer heights and distances. The tracked view positions are interpolated either with a constant height/distance per projector (third and fourth rows) or with different height/distance per vertex (fifth and sixth rows). Photographs taken with per-vertex interpolation show less distortion with consistent vertical perspective across the entire image, and the untracked center view is not affected by the nearby left viewer. Photographs with per-projector interpolation exhibit multiple incorrect perspectives with warped lines and image tearing, and the untracked center view is distorted by the nearby left viewer. The local weight falloff of each tracked position is implemented as either a normalized Gaussian (third and fifth rows) or sharp step hat function (fourth and sixth rows). Gaussian interpolation errors appear as incorrect curved lines while errors using a sharp hat falloff result in an image tearing.

These errors also depend on the shape of the weight falloff function. Using per-projector Gaussian weights (row 5) makes straight lines curved while a per-projector step hat function (row 6) causes image tearing as the view abruptly changes from one vertical height to another. The distortion is less visible on organic objects such as a face, although the left and right eyes are no longer looking in the same direction. Additional results at the start of Video 5 show how this distortion ripples across the geometry as the camera moves back and forth between two tracked projector positions.

Another advantage of per-vertex interpolation is that it reduces errors for untracked viewers. Untracked viewers see the 3-D scene based on a default height and distance that should not be affected by the vertical movement of nearby tracked viewers. Despite the fact that each projector frame may be seen by multiple viewers, by computing multiple vertical perspectives within each projector frame (per-vertex)

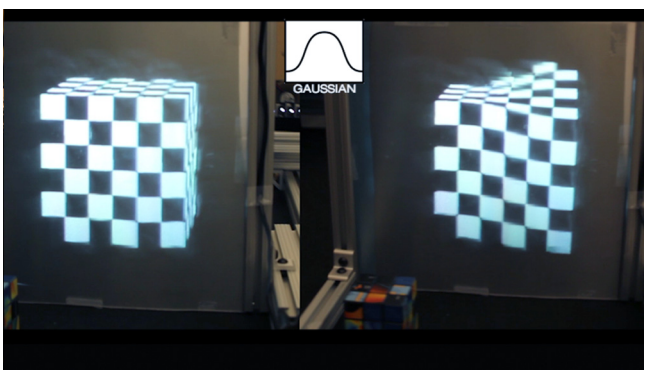

Video 5 Assuming a constant viewer height per projector frame causes image tearing and distortion (right). Per-vertex height interpolation allows for a consistent perspective (left) [URI: http://dx.doi.org/10.1117/1.JEI.23.1.011005.5].

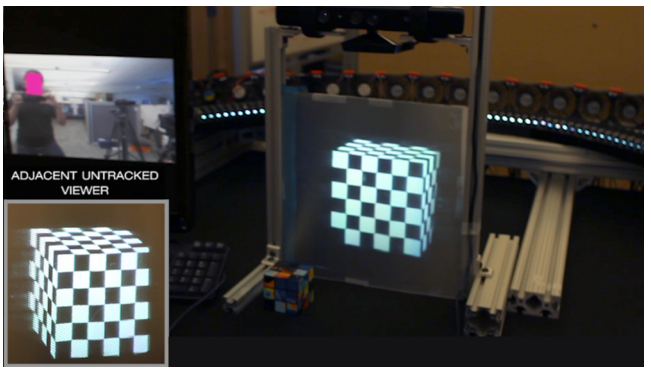

Video 6 This video shows a dynamic tracked viewer in close proximity to an untracked viewer. Per-vertex height interpolation reduces crosstalk between the viewers [URI: http://dx.doi.org/10.1117/1.JEI.23.1.011005.6].

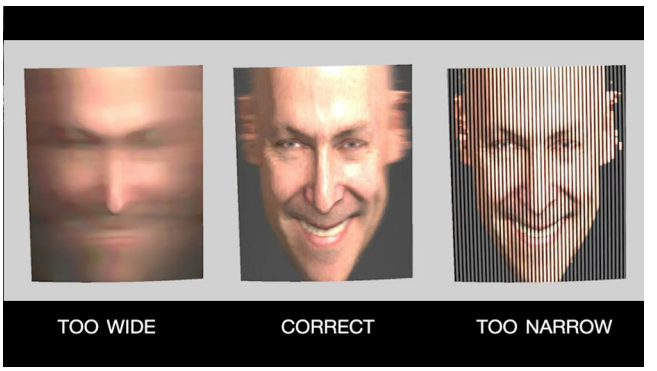

Video 7 Simulation of screens with different levels of horizontal diffusion. The ideal horizontal diffusion should match the angular spacing between projectors [URI: http://dx.doi.org/10.1117/1.JEI.23.1.011005.7].

we can isolate each viewer (Fig. 8, rows 5 and 6). In contrast, the center view of the face appears distorted when interpolating a single height per projector, as this untracked view shares some projectors with the nearby lower left camera (rows 3 and 4). The same effect is shown for a dynamic user in the accompanying video. Without per-vertex interpolation (Video 6, time 0:14), the untracked viewer is clearly distorted whenever the tracked viewer is nearby. At the start of Video 6, this extraneous crosstalk is considerably reduced with per-vertex interpolation.

There is no limit to how many untracked people can view the display simultaneously, as it generates dense horizontal autostereoscopic imagery. However, when viewers start to occlude each other, we cannot completely isolate each viewer's vertical perspective. If two tracked viewers completely overlap or stand right above each other, then their average height and distance are used. An alternative solution to resolving conflicts would be to give higher confidence to nearer viewers so their heights have precedence. For all the results shown in this paper, the width of the Gaussian and hat interpolation functions was 10 deg, which approximates the width of a viewer's shoulders. A wider interpolation falloff provides a horizontal buffer with similar vertical perspective. This is particularly useful if the tracking algorithm has high latency and cannot keep up with sudden horizontal head movements. In contrast, a narrower interpolation falloff further reduces interference when a tracked user is looking over another tracked user's shoulder. As the number of users increases, the tracking system also produces lower confidence values. The current Kinect device is limited to tracking up to six active viewers. In the worst case, the system reverts back to a standard autostereoscopic display with only horizontal parallax.

We test our projection algorithm on a curved mirror with a 10-deg curvature and a magnification factor of 1.43. Figure 9 shows imagery on the curved mirror with and without per-vertex vertical parallax interpolation. In the latter case, perspective distortion increases significantly. This distortion could be reduced by using a wider Gaussian function so that nearby frames would be forced to have similar heights, but this would have the negative effect of more cross talk with nearby viewers. To validate our projection model for a wider range of screen shapes, we implemented a projector array simulator that can model arbitrary screen curvature and diffusion materials. The simulator uses the same render engine but projects onto a screen with a simulated anisotropic BRDF. As shown in the accompanying video (Video 7), we can maintain a stable image with correct perspective as a mirror shape changes significantly. We can also determine the ideal horizontal diffusion width by simulating different anisotropic reflectance lobes.

8 Future Work

In our work, we treat the tracking algorithm as a black box. Future advances in facial tracking will continue to reduce latency and be able to track more viewers over a larger view volume. Knowledge of viewer positions has other applications beyond correcting for vertical parallax. For example, viewing positions can be used to optimize various forms of computational displays or take advantage of stereoperceptual metrics. We are looking to find ways to accelerate the rendering of large numbers of views—for example, large

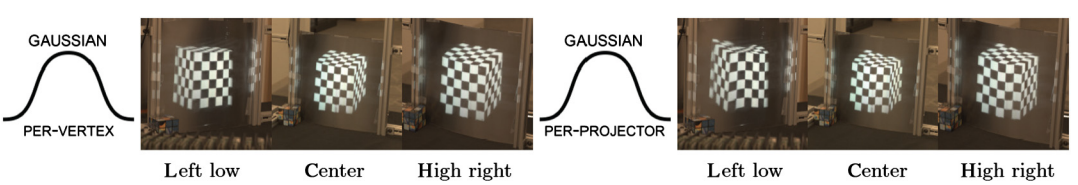

Fig. 9 Comparison of different viewer interpolation functions for a convex mirror. The left set uses per-vertex viewer height and distance with a Gaussian falloff. The right set uses constant height and distance per projector with a Gaussian falloff. Photographs taken with per-vertex interpolation show less distortion with consistent vertical perspective. In contrast, straight lines appear curved in photographs using constant per-projector interpolation.

parts of the rendering pipeline do not need to repeated for every view. Even on modern hardware, rendering 70+ simultaneous views limits scene complexity. An alternative solution would be to distribute rendering across multiple devices. In the extreme case, each projector could have a dedicated low-cost single-board computer such as Raspberry Pi. This could decrease costs, but makes it more difficult to synchronize frames and share resources.

Finally, we plan to adapt our tracking interpolation to other autosteroscopic displays including larger-scale projector arrays. As our display system contains no moving parts, there is no inherent limit to the size of the display. The lenticular and holographic diffuser materials are available in large sheets or rolls. As the display size increases, the projectors will need to be brighter with higher pixel resolution to maintain image quality. It is also possible to scale the field of view. For example, if additional projectors were mounted in a full circle around a cylindrical anisotropic screen, then the display could provide a complete 360-deg viewing experience.

9 Conclusion

In this work, we have shown a new hybrid approach that can display 3-D objects with correct horizontal and compelling perspective from any view. Our new 3-D projector array generates autostereoscopic horizontal parallax with multiuser tracking for vertical parallax. Our display produces full color, no horizontal latency, and a wide field of view that can accommodate a large number of viewers. Our system is reproducible with off-the-shelf projectors, screen materials, graphics cards, and video splitters. Unlike previous 3-D display techniques, we directly render MCOP images with varying horizontal and vertical parallax for every projector. Even though each user sees slices of multiple projectors, the perceived 3-D image is consistent and smooth from any vantage point. Without this method, users experience significant cross talk and geometric distortion particularly when multiple viewers are in close proximity. This rendering framework frees us to explore different projector configurations including front- and rear-mounted projector arrays and nonflat screens. We envisage that this will enable a range of new multiuser applications from live teleconferencing to immersive virtual scenes.

Acknowledgments

We thank the following people for their support and assistance: Bill Swartout, Randall Hill, and Randolph Hall. This work was sponsored by the University of Southern California Office of the Provost, U.S. Air Force DURIP, and U.S. Army Research, Development, and Engineering Command (RDECOM). The content of the information does not necessarily reflect the position or the policy of the U.S. government, and no official endorsement should be inferred.

References

1. A. Jones et al., "Rendering for an interactive 360 light field display," *ACM Trans. Graphics* **26**(3), 40:1–40:10 (2007).
2. A. Jones et al., "Achieving eye contact in a one-to-many 3D video teleconferencing system," *ACM Trans. Graphics* **28**(3), 64:1–64:8 (2009).
3. H. Urey et al., "State of the art in stereoscopic and autostereoscopic displays," *Proc. IEEE* **99**(4), 540–555 (2011).
4. H. Ives, "The projection of parallax panoramagrams," *J. Opt. Soc. Am.* **21**(7), 397–409 (1931).
5. W. Matusik and H. Pfister, "3D tv: a scalable system for real-time acquisition, transmission, and autostereoscopic display of dynamic scenes," *ACM Trans. Graphics* **23**(3), 814–824 (2004).
6. T. Rodriguez et al., "Holographic and action capture techniques," in *SIGGRAPH '07' ACM SIGGRAPH 2007 Emerging Technologies*, K. Ryall and J. Sibert, Eds., Article 11, ACM, New York, NY, USA (2007).
7. P. T. Kovacs and F. Zilly, "3D capturing using multi-camera rigs, real-time depth estimation and depth-based content creation for multi-view and light-field auto-stereoscopic displays," in *SIGGRAPH '12 ACM SIGGRAPH 2012 Emerging Technologies*, P. Smith, Ed., Article 1, ACM, New York, NY (2012).
8. M. Kawakita et al., "3D image quality of 200-inch glasses-free 3D display system," *Proc. SPIE* **8288**, 82880B (2012).
9. S. Yoshida, M. Kawakita, and H. Ando, "Light-field generation by several screen types for glasses-free tabletop 3D display," in *3DTV Conf.: The True Vision-Capture, Transmission and Display of 3D Video (3DTV-CON), 2011*, U. Güdükbay and L. Onural, Eds., pp. 1–4, IEEE, Antalya, Turkey (2011).
10. C. Cruz-Neira, D. J. Sandin, and T. A. DeFanti, "Surround-screen projection-based virtual reality: the design and implementation of the cave," in *Proc. of the 20th Annual Conf. on Computer Graphics and Interactive Techniques, SIGGRAPH '93'*, J. Kajiya, Ed., pp. 135–142, ACM, New York, NY (1993).
11. W. Krger et al., "The responsive workbench," *IEEE Comput. Graphics Appl.* **14**(14), 12–15 (1994).
12. C. Ware, K. Arthur, and K. S. Booth, "Fish tank virtual reality," in *Proc. of the INTERACT '93 and CHI '93 Conf. on Human Factors in Computing Systems, CHI '93'*, S. Ashlund et al., Eds., pp. 37–42, ACM, New York, NY (1993).
13. K. Perlin, S. Paxia, and J. S. Kollin, "An autostereoscopic display," in *Proc. of the 27th Annual Conf. on Computer Graphics and Interactive Techniques, SIGGRAPH '00'*, K. Akeley, Ed., pp. 319–326, ACM Press/Addison-Wesley Publishing Co., New York, NY (2000).
14. J. Jurik et al., "Prototyping a light field display involving direct observation of a video projector array," in *Computer Vision and Pattern Recognition Workshops (CVPRW), 2011 IEEE Computer Society Conf. on*, N. Pinto, Ed., pp. 15–20, IEEE, Colorado Springs (2011).
15. E. Woods, P. Mason, and M. Billinghurst, "Magicmouse: an inexpensive 6-degree-of-freedom mouse," in *GRAPHITE 2003 Proc. of the 1st Int. Conf. on Computer Graphics and Interactive Techniques in Australasia and South East Asia*, M. Adcock, I. Gwilt, and L. Yong Tsui, Eds., pp. 285–286, ACM, New York, NY (2003).
16. P. Rademacher and G. Bishop, "Multiple-center-of-projection images," in *Proc. of the 25th Annual Conf. on Computer Graphics and Interactive Techniques, SIGGRAPH '98'*, H. Rushmeier, Ed., pp. 199–206, ACM, New York, NY (1998).
17. M. Zwicker et al., "Antialiasing for automultiscopic 3D displays," in *Proc. 17th Eurographics Conference on Rendering Techniques EGSR'06*, T. Akenine-Möller and W. Heidrich, Eds., pp. 73–82, Eurographics Association Aire-la-Ville, Switzerland, Switzerland (2006).

Andrew Jones has been a researcher at the USC Institute for Creative Technologies since 2002. His research focus has been on the acquisition and display of realistic content. Previous publications have covered scanning of cultural heritage sites, high-dynamic-range photography, image-based relighting, and recording human shape and motion. He is currently finishing his PhD on autostereoscopic displays including both motorized spinning mirror displays and dense projector arrays.

Koki Nagano is a second-year PhD student in the Computer Science Department at USC. His study of interests lies in 3-D displays and facial animation. He received the BS degree from Tokyo Institute of Technology, Japan, in 2012.

Jing Liu is a third-year PhD student in computer science at UC Santa Cruz. His primary research interests are computational display and photography. He got a BS degree in computer software from Tsinghua University, China, and worked as an intern at Google, the ICT Graphics Lab, and NVIDIA.

Jay Busch has been a technical artist at the USC Institute for Creative Technologies for over 5 years and has been involved in projects such as the Emily Project and the 3-D Teleconferencing System. She graduated with a BS degree in media arts and animation with a side of game design and film production from the Art Institute of Los Angeles in 2007. Her interests run from computer graphics and art to mechanical engineering and prototyping.

Xueming Yu is a researcher at the USC Institute for Creative Technologies. His interest includes engineering of electrical circuit design, mechanics, control system, and researching in real-time

video/audio signal process. He received an MS degree in computer science from University of Southern California and a BS degree in electrical engineering from Shanghai Jiao Tong University.

Mark Bolas is an associate director at the USC Institute of Creative Technologies and an associate professor at the USC School of Cinematic Arts. His work focuses on creating engaging and memorable virtual environments. He holds more than 20 patents and is the recipient of numerous product awards and an IEEE Virtual Reality Technical Achievement Award. His thesis work at Stanford was among the first efforts to map the breadth of virtual reality as a medium.

Paul Debevec is a research professor at the University of Southern California and associate director of graphics research at USC's Institute for Creative Technologies. His publications and animations have focused on image-based rendering, high-dynamic-range imaging, reflectance measurement, facial animation, image-based lighting, and 3-D displays. He serves as the vice president of ACM SIGGRAPH and received a Scientific and Engineering Academy Award in 2010 for his work on the Light Stage facial capture systems.